

Heart Rate Estimation in Photoplethysmogram Signals using Nonlinear Model-Based Preprocessing

Federico Wadehn¹, Yue Zhao², Hans-Andrea Loeliger¹

¹ Signal and Information Processing Laboratory, Department of Electrical Engineering, ETH Zurich, Switzerland

² Department of Electrical Engineering, Tsinghua University, Beijing, China

Abstract

We propose a frequency domain algorithm for heart rate estimation from photoplethysmographic signals (PPG) recorded during intense physical activity. Starting from the Beer-Lambert law we model the effect of movement artifacts on the PPG signal as an amplitude modulation. Using tri-axis accelerometer recordings to demodulate the PPG signal, we are able to extract the heart rate even when motion artifacts are within the frequency band of interest. The average heart rate error using two-channel PPG recordings from 12 subjects was 1.6 BPM with a standard deviation of 3 BPM.

1. Introduction

With the advent of mobile health monitoring devices, long time monitoring of cardiac signals is increasingly being used outside the clinical setting, e.g. for athletic performance evaluation. One of the most popular technologies to monitor cardiovascular activity is pulse oximetry, a non-invasive method based on the change of optical properties of tissue caused by the pulsatile flow of blood during the cardiac cycle. Monitoring the heart rate with wrist-worn pulse oximeters during physical activity features the challenge of signals that are heavily contaminated by motion artifacts (MA). These disturbances often lie within the frequency range of the heart rate, such that simple bandpass filtering for removing motion artifacts is often not enough or even detrimental. In [1] it is suggested to use the independent component analysis to separate motion artifacts from the signal of interest. This approach is well suited for pulse oximetry on the fingertip, where small non-periodic movements like finger bending disrupt the signal. When measuring heart rates with wrist-worn pulse oximeters during physical activity such as running, which is often accompanied by periodic hand swings, the signal should not be seen as a linear superposition of the signal of interest with independent noise signals, as we will show in the

next section. The major drawback of integrating a pulse oximeter into a watch is that the contact between the sensors (LED and photodiode) and the skin is not always guaranteed. In addition, it is much harder to shield wrist-worn pulse oximeters from ambient light compared to fingertip oximeters, due to the loose way of wearing wristbands. In fingertips and earlobes most of the blood vessels are capillaries, compared to the radial artery and veins in the wrist, which are much more affected by motion induced blood movements. A reliable heart rate estimation is usually performed by a series of preprocessing steps to remove motion artifacts followed by an estimation of the power spectral density (PSD) to get the heart rate [2]. The PPG signal consists of quasi-periodic pulses, which are rather peaked as shown in Fig. 1 and are thus only poorly modeled with a pure sinusoid, which though is the underlying assumption in spectral estimation. Other methods to reduce motion artifacts work by correlating the signal with a bank of matched filters to exclude abnormal pulse shapes [3]. After the PPG signal has been “cleaned” to a satisfactory degree, usually some form of spectral estimation is performed to extract the average heart rate from the PPG signal. Using frequency domain methods such as the short-time Fourier transformation has proven to be a robust technique, because by using a window of e.g. 8s, multiple heart beats are captured. Thereby the method is less susceptible to a few abnormal beats or short parts of the signal which are affected by heavy motion artifacts.

In this paper we present an algorithm for heart rate estimation that works both with PPG signals and tri-axis accelerometer data from an inertial measurement unit (IMU) attached to the wrist-worn pulse oximeter. Starting from the Beer-Lambert law, we model the MA-free PPG signal with an exponential of a sinusoid, whose frequency corresponds to the heart rate (cf. Fig. 1). This model allows us further to treat the amplitude modulated PPG signal contaminated by MA as an additive mixture of sinusoids in the log-domain.

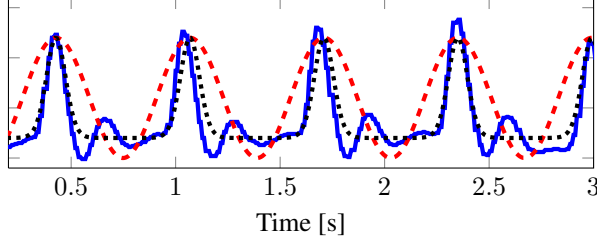


Figure 1. Fitting an exponential of a sinusoid (black dotted) and a pure sinusoid (red dashed) to the PPG signal (blue)

2. Signal Model and Heart Rate Estimation

The Beer-Lambert law [4] describes the attenuation of light traveling through optical media. It states that the received intensity decays exponentially with the traveled path length and the absorption coefficient. Therefore we approximate the PPG signal corresponding to a heart rate of ω_{HR} , with

$$\tilde{y}_{PPG}(t) = \exp(A_1 \sin(\omega_{HR}t + \phi) + A_2), \quad (1)$$

which assumes a uniform heart rate, constant amplitude A_1 and a constant offset A_2 of the log domain signal on the considered window. Fig. 1 suggests to model the PPG signal due to its peakedness rather as an exponential of a sinusoid than as a pure sinusoid. Motion artifacts on the raw PPG data can be caused by two fundamentally different types of motion. On the one hand physical activity such as running is usually accompanied by periodic movements such as hand swings, which influence both the blood flow and the sensor's distance to the skin. Such motion artifacts often lie in the frequency band of interest and have clearly distinguishable frequency components (cf. Fig. 3). On the other hand boxing movements for instance, are abrupt and aperiodic and cause heavy distortions in the PPG signal (cf. Fig. 4), and therefore have to be handled differently. In the case of periodic motion artifacts we model the signal on the accelerometer channels by a sinusoid:

$$a_i(t) = \alpha_i \sin(\omega_i t + \phi_i) + k_i, \quad (2)$$

with $i \in \{x, y, z\}$ and the final signal recorded by the sensor is modeled as:

$$\log(y_{PPG}(t)) = \log(\tilde{y}_{PPG}(t)) + w_x a_x(t) + w_y a_y(t) + w_z a_z(t) \quad (3)$$

in the log-domain. The weighting coefficients w_x, w_y, w_z describe the strength of coupling between the sensor and the accelerometer in a specific direction. Since an addition in the log domain corresponds to a multiplication in the original domain, the peaks in the power spectrum of the

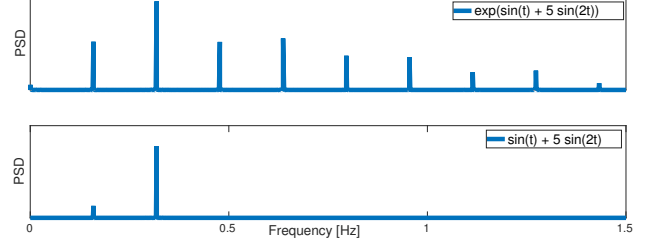


Figure 2. Taking the exponential of the sum of two sinusoids results in an amplitude modulation causing additional spectral peaks.

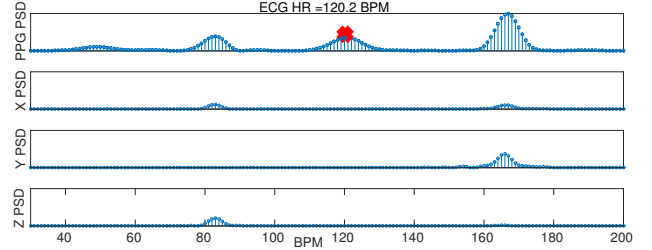


Figure 3. PSD of PPG signal (top), PSD of the tri-axis accelerometer signals. The red cross indicates the real heart rate.

recorded amplitude modulated signal should lie in the set Ω with

$$\Omega = \{\omega_{HR}, \omega_{Ax}, \omega_{Ay}, \omega_{Az}, \\ |\omega_{HR} - \omega_{Ax}|, |\omega_{HR} - \omega_{Ay}|, |\omega_{HR} - \omega_{Az}|, \\ |\omega_{HR} + \omega_{Ax}|, |\omega_{HR} + \omega_{Ay}|, |\omega_{HR} + \omega_{Az}|\}$$

and thus resulting in a smeared spectrum as shown in Fig. 2. Periodic hand swings are usually characterized by translational motion along a specific direction. Therefore, as shown in Fig. 3, the peaks in the power spectra of the accelerometer can be found on all three axis due to the projection of the acceleration vector onto each axis. These spectral peaks also appear in the spectrum of the PPG signal and can exceed in magnitude the spectral peak corresponding to the heart rate.

2.1. Heart Rate Estimation Algorithm

To get the heart rate from the two-channel PPG signal we employed a series of preprocessing steps, followed by a spectral estimation. Firstly, each PPG signal is subdivided into 8s long segments, guaranteeing a sufficient number of samples for the desired frequency resolution.

Secondly, a channel evaluation step to ensure both PPG channels are reliable was employed as follows: If the ratio of the two PPG signal energies is between 1/10 and 10 (of the same order of magnitude), then both channels are assumed to be reliable. Otherwise if the energy in the chan-

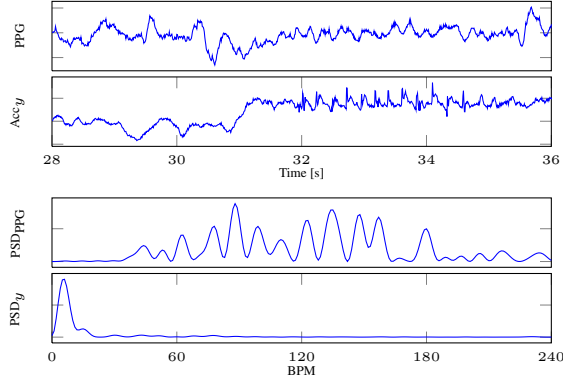


Figure 4. PPG signal with aperiodic motion artifacts

nel with the smaller energy content is larger than an empirically determined threshold, this channel was chosen. A very large energy in the recorded light intensity indicates a loosely attached pulse oximeter, such that a large fraction of the light is reflected directly on the skin surface and thus will not contain any information about the heart rate. A lower bound on the PPG signal energy was used to ensure that the sensor picks up a minimum light intensity. This empirical channel selection is tailored to reflectance-mode pulse oximetry and would not make sense for transmission pulse oximetry, where reflection on the skin surface would reduce the signal's intensity at the receiver.

Following this, the signal in the considered window is bandpass filtered with a 4-th order Butterworth bandpass filter with lower and upper cutoff of 30 BPM and 400 BPM. The upper cutoff is significantly higher than the highest expected heart rate not to distort the PPG signal, because the pulse shape of the PPG signal is more peaked than a sine wave with the same frequency.

One major problem with abrupt movements is the presence of artifacts with a significantly higher amplitude compared to the rest of the signal. The power spectra containing such peaks are completely "smeared" out and often lead to wrong heart rate estimates (c.f. Figure 4). One way to attenuate such spurious spikes is to pass the bandpass filtered PPG signal through a sigmoid function like the $\text{atan}(\cdot)$, which is a bounded function. This way, too high amplitudes will be attenuated and the contamination of the power spectrum due to movement artifacts will be reduced. As a final preprocessing step the logarithm of the non-negative PPG signal is taken to obtain a quasi-periodic signal which resembles more a sinusoid. Given the preprocessed signal we performed a spectral estimation using Goertzel's algorithm with zero-padding to obtain a frequency resolution of 1 BPM. Furthermore we also computed the power spectra of the accelerometer signals to find the frequency peaks of the motion artifacts. When the sum of energies in the 3-axis acceleration signals is larger than

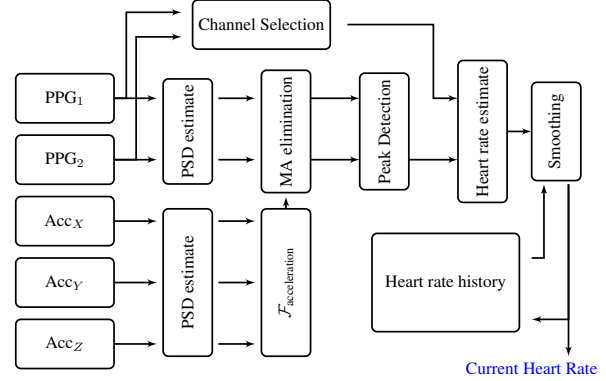


Figure 5. Block diagram of heart rate estimation algorithm after the PPG signal has been preprocessed.

an empirically determined threshold, indicating strong motion artifacts, we used the motion artifact correction. This is done by selecting the peaks $\mathcal{F}_{\text{acceleration}}$ of the PSD of the acceleration signals. The requirements for a peak to be chosen were firstly, at least 30% in amplitude compared to the highest peak and secondly at most 4 peaks were chosen. The spectral components of the PPG signal with frequencies corresponding to peaks in the accelerometer power spectra were multiplied with a rectangular window of width 5 BPM and a weight inversely proportional to the accelerometer PSD peaks' magnitude. Then the peak in the processed power spectrum of the PPG signal was chosen to be the heart rate. The final heart rate estimate is further smoothed with a median filter using the previous 3 heart rate estimates. Following a smoothness condition ($\text{HR changes} < 20 \text{ BPM}$) the heart rate is either set to the spectral peak or the previous heart rate. Fig. 5 shows the core algorithm (with the omission of the preprocessing steps).

3. Performance Metrics

The test data used to benchmark the developed algorithm was taken from [2]. In this trial two-channel PPG signals of 12 subjects in the age range of 19 to 58 years performing various intense physical tasks such as running, push-up or boxing movements were recorded. Simultaneously to the PPG signal a tri-axis accelerometer signal was recorded. The data also contained ECG signals used as a gold-standard for evaluating the algorithm's performance. All signals were recorded using wrist-type pulse oximeters with a wavelength of 609 nm using a sampling rate of 125 Hz. One constraint for the algorithm was that for the estimation of the current heart rate only current and past observations were allowed such that the algorithm can be used for real time applications. One important performance index is the averaged absolute estimation error of the heart

Dataset	μ_{HR}	σ_{HR}	Exercise
1	1.3	2.1	1
2	1.2	3.1	2
3	0.7	1.0	2
4	0.9	1.8	2
5	0.7	1.2	2
6	1.3	2.2	2
7	1.3	1.9	2
8	0.5	0.7	2
9	0.4	0.7	2
10	3.6	6.7	2
11	0.9	1.3	2
12	6.6	14.2	2

Table 1. Absolute estimation error and standard deviation of the absolute error for the 12 training subjects.

rate which is defined as:

$$\mu_{HR} = 1/W \sum_{i=1}^W |HR_{est}(i) - HR_{true}(i)|, \quad (4)$$

where W is the total number of heart rate estimates, where $HR_{est}(i)$ is the i -th PPG heart rate estimate, and where $HR_{true}(i)$ is the i -th ground-truth heart rate from the ECG. A second index we considered is σ_{HR} , the standard deviation of the absolute estimation error of the heart rate. To visually inspect the performance of the developed algorithm we used the Bland-Altman plots, to see in which heart rate region the performance of the algorithm was strong and in which parts of the signal the performance was poor.

4. Results

Table 1 shows the average absolute estimation error, the standard deviation of the absolute estimation error and the exercise protocol as described in [2] for each of the 12 training subjects. The average heart rate estimation error for the first 12 subjects running on the treadmill is 1.6 BPM (2.3 BPM was achieved in [2]). An additional recording provided by Z. Zhang from [2] had an average estimation error of 9.6 BPM and a standard deviation of the absolute estimation error of 17 BPM. This could be due to the different types of exercises, which were performed, that unlike running did not result in periodic movement artifacts. In Fig. 6 we can visually inspect how well the heart rate estimation using the PPG signal matches the heart rate extracted from the ECG signal for all 12 training subjects.

5. Discussion and Conclusion

We presented an algorithm for estimation of heart rates from photoplethysmographic signals recorded during intense physical exercise. The algorithm is based on spectral

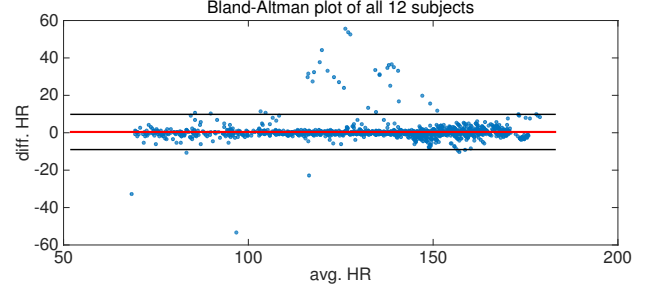


Figure 6. Bland-Altman plot of estimated heart rate from ECG and PPG for all 12 training subjects.

estimation, preceded by a cascade of nonlinear preprocessing steps, which include knowledge obtained from the accelerometers. The choice of the window size on which to estimate the heart rate is an important question. A larger window will contain more heart beats and therefore tends to be more robust, due to its ability to discard small contaminated parts of the signal. Due to heart rate variability on the other hand choosing a too large window will result in a very crude estimate of the heart rate. The main weakness of frequency based approaches is the assumption of a uniform heart rate, which is surely violated, especially when performing intense physical exercise. The algorithm has a very low average error rate when motion artifacts are periodic such as they occur when running. When dealing with motion artifacts such as abrupt movements in boxing, the algorithm had an inferior performance.

References

- [1] B. S. Kim and S. K. Yoo, "Motion artifact reduction in photoplethysmography using independent component analysis," *IEEE Transactions on Biomedical Engineering*, vol. 53, no. 3, pp. 566–568, 2006.
- [2] Z. Zhang, Z. Pi, and B. Liu, "Troika: A general framework for heart rate monitoring using wrist-type photoplethysmographic signals during intensive physical exercise," *IEEE Transactions on Biomedical Engineering*, vol. 62, no. 2, pp. 522–531, 2015.
- [3] F. Wadehn, D. Carnal, and H.-A. Loeliger, "Estimation of heart rate and heart rate variability from pulse oximeter recordings using localized model fitting," in *Engineering in Medicine and Biology Society (EMBC), Annual International Conference of the IEEE*, Aug. 2015.
- [4] R. Graaff, A. Dassel, W. Zijlstra, F. De Mul, and J. Aarnoudse, "How tissue optics influences reflectance pulse oximetry," *Oxygen Transport to Tissue XVII*, Springer, 1996.

Address for correspondence:

Federico Wadehn, wadehnf@isi.ee.ethz.ch
8092 Zurich,
Switzerland